

NUCLEAR DATA AND MEASUREMENTS SERIES

ANL/NDM-85

**Measurement of the $^{51}\text{V}(\text{n,p})^{51}\text{Ti}$ Reaction Cross Section from
Threshold to 9.3 MeV by the Activation Method**

by

Donald L. Smith, James W. Meadows, and Ikuo Kanno

June 1984

**ARGONNE NATIONAL LABORATORY,
ARGONNE, ILLINOIS 60439, U.S.A.**

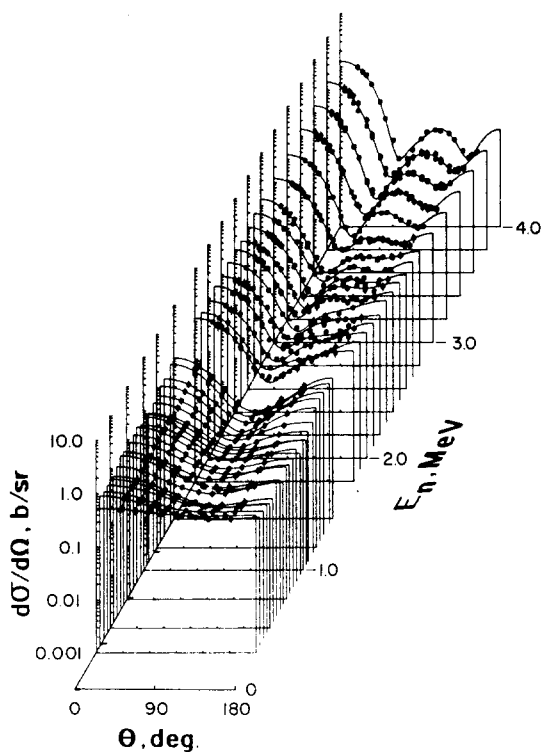
NUCLEAR DATA AND MEASUREMENTS SERIES

ANL/NDM-85

MEASUREMENT OF THE $^{51}\text{V}(n,p)^{51}\text{Ti}$ REACTION CROSS SECTION FROM THRESHOLD TO 9.3 MeV BY THE ACTIVATION METHOD*

by

Donald L. Smith, James W. Meadows and Ikuo Kanno**
June 1984



ARGONNE NATIONAL LABORATORY,
ARGONNE, ILLINOIS 60439, U.S.A.

The facilities of Argonne National Laboratory are owned by the United States Government. Under the terms of a contract (W-31-109-Eng-38) among the U. S. Department of Energy, Argonne Universities Association and The University of Chicago, the University employs the staff and operates the Laboratory in accordance with policies and programs formulated, approved and reviewed by the Association.

MEMBERS OF ARGONNE UNIVERSITIES ASSOCIATION

The University of Arizona	The University of Kansas	The Ohio State University
Carnegie-Mellon University	Kansas State University	Ohio University
Case Western Reserve University	Loyola University of Chicago	The Pennsylvania State University
The University of Chicago	Marquette University	Purdue University
University of Cincinnati	The University of Michigan	Saint Louis University
Illinois Institute of Technology	Michigan State University	Southern Illinois University
University of Illinois	University of Minnesota	The University of Texas at Austin
Indiana University	University of Missouri	Washington University
The University of Iowa	Northwestern University	Wayne State University
Iowa State University	University of Notre Dame	The University of Wisconsin-Madison

NOTICE

This report was prepared as an account of work sponsored by the United States Government. Neither the United States nor the United States Department of Energy, nor any of their employees, nor any of their contractors, subcontractors, or their employees, makes any warranty, express or implied, or assumes any legal liability or responsibility for the accuracy, completeness or usefulness of any information, apparatus, product or process disclosed, or represents that its use would not infringe privately-owned rights. Mention of commercial products, their manufacturers, or their suppliers in this publication does not imply or connote approval or disapproval of the product by Argonne National Laboratory or the U. S. Department of Energy.

ANL/NDM-85

MEASUREMENT OF THE $^{51}\text{V}(n,p)^{51}\text{Ti}$ REACTION CROSS
SECTION FROM THRESHOLD TO 9.3 MeV BY THE
ACTIVATION METHOD*

by

Donald L. Smith, James W. Meadows and Ikuo Kanno**
June 1984

E NUCLEAR REACTION $^{51}\text{V}(n,p)^{51}\text{Ti}$. Measured $\sigma_{np}(E_n)$,
 $E_n = 2.856 - 9.267$ MeV. Activation method. Counted
0.320-MeV ^{51}Ti decay gamma rays. Measured ^{51}Ti half life.
Standard: ENDF/B-V $\sigma_f(E_n)$ for ^{238}U . Detailed uncertainty
analysis. Integral-differential comparisons for ^{252}Cf and
 ^{235}U fission-neutron spectra.

Applied Physics Division
Argonne National Laboratory
9700 South Cass Avenue
Argonne, Illinois 60439
USA

*This work supported by the U.S. Department of Energy.

**Exchange Associate. Permanent Address:
Research Reactor Institute, Kyoto University
Kumatori-Cho, Sennan-Gun, Osaka 590-04
Japan.

NUCLEAR DATA AND MEASUREMENTS SERIES

The Nuclear Data and Measurements Series presents results of studies in the field of microscopic nuclear data. The primary objective is the dissemination of information in the comprehensive form required for nuclear technology applications. This Series is devoted to: a) measured microscopic nuclear parameters, b) experimental techniques and facilities employed in measurements, c) the analysis, correlation and interpretation of nuclear data, and d) the evaluation of nuclear data. Contributions to this Series are reviewed to assure technical competence and, unless otherwise stated, the contents can be formally referenced. This Series does not supplant formal journal publication but it does provide the more extensive information required for technological applications (e.g., tabulated numerical data) in a timely manner.

INFORMATION ABOUT OTHER ISSUES IN THE ANL/NDM SERIES:

A list of titles and authors for reports ANL/NDM-1 through ANL/NDM-50 can be obtained by referring to any report of this series numbered ANL/NDM-51 through ANL/NDM-76. Requests for a complete list of titles or for copies of previous reports should be directed to:

Section Secretary
Applied Nuclear Physics Section
Applied Physics Division
Building 316
Argonne National Laboratory
9700 South Cass Avenue
Argonne, Illinois 60439
USA

- ANL/NDM-51 Measured and Evaluated Neutron Cross Sections of Elemental Bismuth by A. Smith, P. Guenther, D. Smith and J. Whalen, April 1980.
- ANL/NDM-52 Neutron Total and Scattering Cross Sections of ${}^6\text{Li}$ in the Few MeV Region by P. Guenther, A. Smith and J. Whalen, February 1980.
- ANL/NDM-53 Neutron Source Investigations in Support of the Cross Section Program at the Argonne Fast-Neutron Generator by James W. Meadows and Donald L. Smith, May 1980.
- ANL/NDM-54 The Nonelastic-Scattering Cross Sections of Elemental Nickel by A. B. Smith, P. T. Guenther and J. F. Whalen, June 1980.
- ANL/NDM-55 Thermal Neutron Calibration of a Tritium Extraction Facility using the ${}^6\text{Li}(n,t){}^4\text{He}/{}^{197}\text{Au}(n,\gamma){}^{198}\text{Au}$ Cross Section Ratio for Standardization by M. M. Bretscher and D. L. Smith, August 1980.
- ANL/NDM-56 Fast-Neutron Interactions with ${}^{182}\text{W}$, ${}^{184}\text{W}$ and ${}^{186}\text{W}$ by P. T. Guenther, A. B. Smith and J. F. Whalen, December 1980.
- ANL/NDM-57 The Total, Elastic- and Inelastic-Scattering Fast-Neutron Cross Sections of Natural Chromium by Peter T. Guenther, Alan B. Smith and James F. Whalen, January 1981.
- ANL/NDM-58 Review of Measurement Techniques for the Neutron Capture Process by W. P. Poenitz, August 1981.
- ANL/NDM-59 Review of the Importance of the Neutron Capture Process in Fission Reactors by Wolfgang P. Poenitz, July 1981.
- ANL/NDM-60 Gamma-Ray Detector Calibration Methods Utilized in the Argonne FNG Group Activation Cross Section Measurement Program by James W. Meadows and Donald L. Smith, April 1984.

- ANL/NDM-61 Fast-neutron Total and Scattering Cross Sections of ^{58}Ni by Carl Budtz-Jørgensen, Peter T. Guenther, Alan B. Smith and James F. Whalen, September 1981.
- ANL/NDM-62 Covariance Matrices and Applications to the Field of Nuclear Data by Donald L. Smith, November 1981.
- ANL/NDM-63 On Neutron Inelastic-Scattering Cross Sections of ^{232}Th , ^{233}U , ^{235}U , ^{238}U , ^{239}U , and ^{239}Pu and ^{240}Pu by Alan B. Smith and Peter T. Guenther, January 1982.
- ANL/NDM-64 The Fission-Fragment Angular Distributions and Total Kinetic Energies for $^{235}\text{U}(n,f)$ from 0.18 to 8.83 MeV by James W. Meadows and Carl Budtz-Jørgensen, January 1982.
- ANL/NDM-65 Note on the Elastic Scattering of Several-MeV Neutrons from Elemental Calcium by Alan B. Smith and Peter T. Guenther, March 1982.
- ANL/NDM-66 Fast-neutron Scattering Cross Sections of Elemental Silver by Alan B. Smith and Peter T. Guenther, May 1982.
- ANL/NDM-67 Non-evaluation Applications for Covariance Matrices by Donald L. Smith, July 1982.
- ANL/NDM-68 Fast-neutron Total and Scattering Cross Sections of ^{103}Rh by Alan B. Smith, Peter T. Guenther and James F. Whalen, July 1982.
- ANL/NDM-69 Fast-neutron Scattering Cross Sections of Elemental Zirconium by Alan B. Smith and Peter T. Guenther, December 1982.
- ANL/NDM-70 Fast-neutron Total and Scattering Cross Sections of Niobium by Alan B. Smith, Peter T. Guenther and James F. Whalen, July 1982.
- ANL/NDM-71 Fast-neutron Total and Scattering Cross Sections of Elemental Palladium by Alan B. Smith, Peter T. Guenther and James F. Whalen, June 1982.
- ANL/NDM-72 Fast-neutron Scattering from Elemental Cadmium by Alan B. Smith and Peter T. Guenther, July 1982.
- ANL/NDM-73 Fast-neutron Elastic-Scattering Cross Sections of Elemental Tin by C. Budtz-Jørgensen, Peter T. Guenther and Alan B. Smith, July 1982.
- ANL/NDM-74 Evaluation of the ^{238}U Neutron Total Cross Section by Wolfgang Poenitz, Alan B. Smith and Robert Howerton, December 1982.

- ANL/NDM-75 Neutron Total and Scattering Cross Sections of Elemental Antimony by Alan B. Smith, Peter T. Guenther and James F. Whalen, September 1982.
- ANL/NDM-76 Scattering of Fast-Neutrons from Elemental Molybdenum by Alan B. Smith and Peter T. Guenther, November 1982.
- ANL/NDM-77 A Least-Squares Method for Deriving Reaction Differential Cross Section Information from Measurements Performed in Diverse Neutron Fields by Donald L. Smith, November 1982.
- ANL/NDM-78 Fast-Neutron Total and Elastic-Scattering Cross Sections of Elemental Indium by A. B. Smith, P. T. Guenther, and J. F. Whalen, November 1982.
- ANL/NDM-79 Few-MeV Neutrons Incident on Yttrium by C. Budtz-Jørgensen, P. Guenther, A. Smith and J. Whalen, June 1983.
- ANL/NDM-80 Neutron Total Cross Section Measurements in the Energy Region from 47 keV to 20 MeV by W. P. Poenitz and J. F. Whalen, July 1983.
- ANL/NDM-81 Covariances for Neutron Cross Sections Calculated Using a Regional Model Based on Elemental-Model Fits to Experimental Data by Donald L. Smith and Peter T. Guenther, November 1983.
- ANL/NDM-82 Reaction Differential Cross Sections from the Least-Squares Unfolding of Ratio Data Measured in Diverse Neutron Fields by D. L. Smith, January 1984.
- ANL/NDM-83 The Fission Cross Sections of Some Thorium, Uranium, Neptunium and Plutonium Isotopes Relative to ^{235}U by J. W. Meadows, October 1983.
- ANL/NDM-84 ^{235}U and ^{239}Pu Sample-Mass Determinations and Intercomparisons by W. P. Poenitz and J. W. Meadows, November 1983.

TABLE OF CONTENTS

	<u>Page</u>
ABSTRACT	-vi-
I. INTRODUCTION	1
II. EXPERIMENTAL PROCEDURE	2
III. DATA ANALYSIS	5
IV. EXPERIMENTAL RESULTS AND DISCUSSION	7
V. INTEGRAL-DIFFERENTIAL COMPARISONS	8
VI. CONCLUSIONS.	10
ACKNOWLEDGEMENTS.	11
REFERENCES.	12
TABLES	17
FIGURES.	27

MEASUREMENT OF THE $^{51}\text{V}(n,p)^{51}\text{Ti}$ REACTION CROSS SECTION FROM
THRESHOLD TO 9.3 MEV BY THE ACTIVATION METHOD*

by

Donald L. Smith, James W. Meadows and Ikuo Kanno**

Applied Physics Division
Argonne National Laboratory
9700 S. Cass Avenue
Argonne, Illinois 60439
U.S.A.

ABSTRACT

The activation method was used to measure cross sections for the $^{51}\text{V}(n,p)^{51}\text{Ti}$ reaction from near threshold at 2.856 MeV up to 9.267 MeV. Forty-five approximately-monoenergetic cross section values were obtained; they provide complete, detailed coverage of this energy range with FWHM resolutions of ~ 0.08 to 0.1 MeV below ~ 4.7 MeV and ~ 0.14 to 0.28 MeV above this energy. These data span $\sim 90\%$ of the total response for the standard ^{235}U thermal-neutron-induced-fission neutron spectrum and $\sim 86\%$ of the total response for the standard ^{252}Cf spontaneous-fission neutron spectrum. The present experimental cross sections are significantly larger (e.g., by $\sim 50\%$ at ~ 8 MeV) than the corresponding values from the ENDF/B-V evaluation which was derived from nuclear model calculations. The calculated integral cross section (based on the present work) for the ^{252}Cf spontaneous-fission neutron spectrum agrees very well with a recently reported measurement (the calculated value is only $\sim 2\%$ smaller). Corresponding agreement with the equivalent experimental value for the ^{235}U thermal-neutron-induced-fission neutron spectrum is less favorable (the calculated value is $\sim 20\%$ larger).

* This work supported by the U. S. Department of Energy.

** Exchange Associate. Permanent Address: Research Reactor Institute, Kyoto University, Kumatori-Cho, Sennan-Gun, Osaka 590-04, Japan.

I. INTRODUCTION

The present experiment was motivated primarily by applied considerations. A survey of CINDA [1] indicated that no experimental neutron-energy-dependent cross section data for the $^{51}\text{V}(n,p)^{51}\text{Ti}$ reaction have been reported for neutron energies below ~ 13 MeV. The Q -value for this reaction is -1.684 MeV which corresponds to a theoretical threshold of 1.717 MeV [2]. Thus, in effect, no experimental cross section data were available for the entire energy range of importance for fast-neutron fission reactors, or for a significant portion of the energy range of interest for fusion-energy applications as well. Data requests for the $^{51}\text{V}(n,p)^{51}\text{Ti}$ reaction have been published (e.g., Refs. 3 and 4). The primary concern involves the radiation damage produced in components of reactors which experience high fluences of fast neutrons. It is known that neutron-radiation-induced hydrogen gas production leads to metallic embrittlement (e.g., Ref. 5). This problem is regarded as potentially quite acute for fusion-energy devices where the average neutron energy is higher, and the vanadium content is likely to be greater, than for fission reactors.

Experimental (n,p) cross sections are of physical interest because they provide a basis for a more comprehensive understanding of systematics of the (n,p) process. In addition to being relevant to nuclear-energy technology, these data can be used to test nuclear reaction models and to provide information on nuclear level densities [6]. $^{51}\text{V}(n,p)^{51}\text{Ti}$ is one of a limited number of (n,p) reactions which can be readily investigated experimentally using conventional activation techniques. In many other instances difficulties are encountered due to factors such as limited availability of isotopic samples, inconvenient decay half lives, and problematic decay schemes. Direct charged-particle emission measurements are difficult and are prone to larger errors than most activation studies (e.g., see Refs. 7-9). Therefore, activation gives more precise results in favorable cases. Applied need for a wide range of (n,p) cross sections, many of which are not measurable or are barely measurable, motivates research on the development of improved models and model parameterizations to be used for calculation. To be reliable, these models must be validated by testing them against experimental data. Clearly, the larger the available data base of accurately-measured (n,p) results, the greater the progress to be expected toward fulfilling this goal. It is evident from recent experience acquired in the development and testing of the ENDF/B-V evaluation that much more work needs to be done in this field [10]. The basic objective of this experiment is the measurement of cross sections for the $^{51}\text{V}(n,p)^{51}\text{Ti}$ reaction from as low a neutron energy as allowed by the experimental sensitivity of our activation method up to the maximum monoenergetic neutron energy routinely accessible in our laboratory ($\gtrsim 9$ MeV). Section II describes the experimental method used in this work. Section III deals with details of the data analysis, including a comprehensive treatment of experimental errors. The results are reported in Section IV, and comparisons are made with other monoenergetic experimental data (all above 13 MeV) and with several existing evaluations for the $^{51}\text{V}(n,p)^{51}\text{Ti}$ reaction. Section V discusses a comparison we have made between available differential and integral results for two widely-employed standard fission-neutron spectra. Finally, our conclusions appear in Section VI.

II. EXPERIMENTAL PROCEDURE

The $^{51}\text{V}(n,p)^{51}\text{Ti}$ reaction is quite amenable to measurement via the activation method. The isotopic abundance of ^{51}V in elemental vanadium is 99.750%, with ^{50}V as the only other isotopic constituent [2]. The decay half life of ^{51}Ti is 348 sec ($\pm 0.5\%$) [2]. This half life, while rather short, is nevertheless manageable for activation measurements, without application of any special techniques. Decay of ^{51}Ti produces a 0.320-MeV gamma ray $93.4 \pm 0.9\%$ of the time [2].

The samples utilized in the present work were fabricated from metallic vanadium. The vanadium content was $99.8 \pm 0.2\%$ by weight. The dominant impurities were Al, Si, Cr and Fe, but none of these were problems insofar as the present experiment was concerned. The sample density was measured as $5.92 \pm 0.04 \text{ g/cm}^3$. All the samples were nearly identical disks averaging 0.330 cm in thickness and 2.557 cm in diameter.

Nearly-monoenergetic neutrons for the irradiations were produced by the method of bombarding thin targets with monoenergetic charged-particle beams from the Argonne National Laboratory Fast-Neutron Generator (FNG) Facility [11,12]. For neutron energies below ~ 4.7 MeV, the $^7\text{Li}(p,n)^7\text{Be}$ reaction was used [13,14]. The targets were thin films of metallic natural lithium metal evaporated onto 0.025-cm-thick tantalum metal backings. The measurements above ~ 4.7 MeV were performed using the $^2\text{H}(d,n)^3\text{He}$ reaction. A gas target, as shown in Fig. 1 and further described in Refs. 15 and 16, was employed. Each of these target assemblies was required to dissipate up to 100 watts of beam power. The lithium targets were oscillated and cooled by an air jet. The gas-target assembly was water cooled and an air jet was also used. The neutron energy was controlled by selecting the appropriate incident-charged-particle energy, since both of the neutron source reactions are two-body reactions with well-defined Q-values. Each source reaction suffers interference from secondary-neutron reactions at higher energies so that neither is truly monoenergetic [13,15]. Methods for coping with this problem have been previously described [13,15,17,18]. The proton and deuteron beams from the FNG accelerator were magnetically analyzed, and the energy scale calibration was based upon observation of the well-known $^7\text{Li}(p,n)^7\text{Be}$ and $^{11}\text{B}(p,n)^{11}\text{C}$ reaction thresholds [19,20]. Although the charged particle energies are probably known to within ± 5 keV over the entire energy range of this experiment, the average neutron energies were less well known, primarily due to uncertainties in calculating target energy losses for the incident charged particles. Thus, the average neutron energies reported in this work are conservatively estimated to be uncertain by about 20% of the full-width-half-maximum (FWHM) resolutions for the incident neutron energy distributions, i.e., by ~ 15 -55 keV.

The cylindrical vanadium samples were each placed perpendicular to the charged-particle beam line (zero degrees) at a distance of 3.964 cm from

the target for the irradiations. These samples were attached to the low-mass fission detector monitor shown in Fig. 1. This detector is a parallel-plate flow-through ionization chamber used to detect fission fragments emitted from a thin deposit of uranium. The chamber itself has 0.025-cm-thick steel walls. The chamber electrode and uranium deposit backing are 0.025-cm-thick steel disks. Methane (CH_4) at atmospheric pressure is the filler gas. The uranium deposit consists of a thin, uniform film of depleted uranium (effectively 100% ^{238}U) 2.54-cm in diameter, amounting to 5.012×10^{18} ($\pm 2\%$) atoms. Procedures for making and calibrating this deposit have been previously described [21-23].

Activity measurements for ^{51}Ti involved counting 0.320-MeV gamma radiation with a Ge(Li) detector having an active volume of $\sim 100 \text{ cm}^3$. Counting deadtime corrections were deduced from information recorded for each count. Each sample was counted in a well-defined position close to this detector. Calibration was ultimately based upon two standard radioactive sources. One source was ^{152}Eu which was obtained from Saclay, France [24]. The second source was a Mixed Radionuclide Standard source from the National Bureau of Standards, U.S.A. [25]. Both of these standards were point sources on thin mylar backings. They were too strong to count in the close geometry used to actually count the irradiated vanadium samples. Furthermore, neither standard source yielded a gamma-ray line near 0.320-MeV where the calibration was desired. Consequently, several experimental and computational steps were required in order to obtain the desired calibration. First, a second reproducible counting position was established $\sim 22 \text{ cm}$ from the detector. Then, the ratio of the counting efficiency for 0.320-MeV ^{51}Ti gamma rays at this distant position to that for counting them at the close-in counting position was measured using typical vanadium samples irradiated to relatively high activity levels. This method automatically takes differences in photon absorption, geometry and detector response for the two positions into account. Next, the ^{152}Eu and Mixed Standard sources were repeatedly counted at the distant position, thereby establishing absolute efficiencies at this defined position for several gamma rays emitted from these sources. Measurements were also made to determine the positioning sensitivity at the distant counting position, to deduce the photon absorption in vanadium, and to look for coherent scattering effects (none were seen). These results were used in calculations which yielded the absolute efficiencies for several standard gamma lines at the distant counting position, assuming that these activities were uniformly distributed in a vanadium sample. These efficiency values vs. photon energy were least-squares fitted with an expansion in powers of the logarithm of photon energy. Several expansion orders were tried, with little improvement in quality of fit observed above fifth order. The efficiency for counting a distributed 0.320-MeV gamma source at the distant position was deduced from this curve. This value, in conjunction with the previously-mentioned, measured close-to-distant efficiency ratio, yielded the final required counting efficiency for the experiment. It should be noted that the two distinct standard gamma-ray sources utilized in this calibration yielded consistent results within their experimental errors. The overall estimated uncertainty for the calibration procedure is $\pm 2.4\%$.

The rather short half life of ^{51}Ti made it necessary to plan the irradiation/count sequence carefully. The fission events and gamma-ray spectra were recorded in multichannel pulse-height analyzers. However, the spectra were partially summed so that only a few numbers had to be recorded rather than complete spectra. This speeded up the data recording process. A window was set on the 0.320-MeV gamma-ray full-energy peak, with equal windows set immediately above and below it. Since no interfering lines were observed in the spectra, these three sums offered a quite reliable means for determining the full-energy peak yield. Typically, each sample was irradiated for ~ 6 minutes and counted for ~ 6 minutes, with ~ 1 minute delay between the end of each exposure and the beginning of each count. The neutron output rate from the target was monitored using a long counter and ratemeter. It was found to be sufficiently constant during each run so as to eliminate the need for recording time profiles and applying related corrections. A companion measurement was made for each main run to provide information on fissions and ^{51}Ti activity produced by background neutrons from the target structures. For the lithium target measurements, a bare tantalum target was substituted for the lithium targets (which contained films of natural lithium metal ~ 200 keV thick for 1.881 MeV protons). The background-induced ^{51}Ti activity was too small to measure for the lithium target studies, and the corresponding background fissions amounted to fewer than 1% at the highest energy. Background measurements for the gas-target irradiations were achieved by evacuating the cell. Most of the background neutrons came from (d,n) reactions with the 3.2 mg/cm²-Nickel-foil cell-entrance window or with impurities which normally build up on the target. The background tends to vary, but only negligibly over the short irradiation-time intervals of the present experiment. We found that the background fissions were in the range 2-30%, while the background ^{51}Ti production was less than 7% at all energies.

We measured the half life for the 0.320-MeV gamma ray activity to insure that it originated from ^{51}Ti decays, free of contamination from different activities. The procedure was as follows: At the high-energy end of our experiment we irradiated a vanadium sample long enough to produce a relatively high level of ^{51}Ti activity. The yield of 0.320-MeV gamma rays per unit livetime of the detection apparatus was then measured in adjacent time intervals over a period exceeding five half lives. These data were least-squares fitted with an exponential, yielding a half life of 351.6 sec ($\pm 1.4\%$). This value agrees very well with the accepted value [2] within the errors. Since the latter has a smaller error, we decide to utilize it in all our analyses rather than our own result.

The counting rates for the vanadium samples were sensitive to the sample orientation ($\sim 3.7\%$ difference). This reflects a nonuniformity of ^{51}Ti activity in the samples, an effect which is to be expected for the irradiation and counting geometries of this experiment. Very careful control was maintained over the irradiation and counting orientations for each sample in this experiment. Owing to the procedure used to calibrate the counting apparatus, the effect of sample activity nonuniformity cancels to first-order

so long as each sample is counted using the same orientation convention as that established in the calibration procedure. This was the case in the present experiment, so no correction was applied to the count data.

III. DATA ANALYSIS

The experimental data were analyzed using the same general methods described in Refs. 15 and 26, although there have been some procedural refinements during the intervening decade.

The first step involved deducing the 0.320-MeV gamma-ray peak yields and their uncertainties for all runs including background ones. Utilizing parameters from the individual radiation histories, corrections for ^{51}Ti activity decay were applied. These results, when combined with the measured Ge(Li) detector efficiency, yielded values for the total number of ^{51}Ti atoms produced during each irradiation. These results were further corrected for detector efficiency. The time-and-efficiency-corrected results were then examined from the point of view of background effects. As mentioned in Section II, background data were recorded for each distinct experimental point.

Next, we examined the fissions data. An extrapolation correction was deduced to account for fission events of low-energy which were masked by the alpha-particle and noise pulses. For the gas target measurements this correction was typically $\sim 4\%$. The higher cutoff used for the lithium target measurements, led to corrections amounting typically to $\sim 8\%$. Fission fragments emitted near 90° in the uranium deposit cannot escape and thus are not recorded. This effect is somewhat energy dependent and it also depends upon the fragment angular distributions. The correction is clearly dependent upon the deposit thickness. Using fragment angular distribution data from Ref. 27 we found that a correction of $\sim 3-4\%$ was required for this effect in our experiment. Corrections for fissions produced by background neutrons were also applied. These corrections were based on data from individual background measurements.

Neutron multiple-scattering corrections could not be measured so they were calculated. The basic concept is described in Ref. 26, but the calculational procedure has since been improved and it is further described in Ref. 28. The scattering probabilities are sufficiently small in experiments such as the present one so that the correction procedure involves calculating only the additional events produced by singly-scattered neutrons. Both elastic and inelastic scattering contributions are included. The scattering-correction parameters were calculated at several neutron energies using ENDF/B evaluated total, scattering and reaction cross sections [10]. The results appear in Table 1. Required values at all energies were derived from this table by linear interpolation. There is some cancellation in the effects of these scattering processes since this is basically a ratio experiment. The net correction, however, amounts to $\sim 5-8\%$ over the energy range of the present investigation.

The corrected measured fission and activity data, and calculated scattering corrections, were utilized to compute $^{51}\text{V}(n,p)^{51}\text{Ti}$ -to- $^{238}\text{U}(n,f)$ cross section ratios. The calculations were performed using computer codes which determine a number of additional corrections involving geometry factors, neutron source properties, neutron absorption, etc. Again, the procedure is basically as described in Refs. 15 and 26, refined to incorporate newer concepts as described in Ref. 17. These newer features deal primarily with the way the average neutron energy and neutron energy resolution are calculated. These are important considerations for the present experiment since the (n,p) cross section is strongly energy dependent near threshold.

Corrections for secondary-neutron groups from the source are a matter of concern. For the lithium source, the $^7\text{Li}(p,n)^7\text{Be}$ and $^7\text{Li}(p,n)^7\text{Be}^*$ reactions produce discrete groups while the $^7\text{Li}(p,n^3\text{He})^4\text{He}$ breakup reaction produces a broad continuous group [13,14]. Features of the $^7\text{Li}(p,n)^7\text{Be}^*$ secondary-neutron reaction are sufficiently well known so that little uncertainty is introduced into the computed cross sections by the corrections for this group. The $^7\text{Li}(p,n^3\text{He})^4\text{He}$ reaction is not so well characterized so it is of interest to examine the effect these neutrons have upon the computed cross sections [11,13]. We determined that neglect of this breakup group would affect the computed cross section by $< 3.4\%$ at all energies of this experiment. Since the correction is actually applied in this work, the uncertainty is believed to be $< 1\%$. There are only two source reactions to consider for the gas-target measurements. The $^2\text{H}(d,n)^3\text{He}$ reaction produces a discrete group while the $^2\text{H}(d,np)^2\text{H}$ reaction produces a continuous breakup group [11,15]. Neglect of the breakup group would effect the computed cross section by $< 8.3\%$ at all energies. However, the breakup correction was applied for gas target measurements as well, so the uncertainty is believed to be $< 2\%$.

When the gas target heats up due to beam-energy deposition, the density of the gas in the cell decreases [16]. This alters the effective energy resolution and leads to slightly higher average neutron energies. We took this effect into consideration in analyzing the data of the present experiment. In the worst case, a shift of < 10 keV toward higher average neutron energy resulted.

We have estimated what we expect are the main error sources for this experiment, including correlations, using methods described in Refs. 29 and 30. The objective of this effort is provision of sufficient uncertainty information so that a complete ratio-data covariance matrix could be generated for evaluation applications (e.g., see Ref. 29). Since this experiment yielded 45 distinct cross section values, explicit representation of the corresponding covariance matrix would involve 990 distinct values. This appeared to us to be impractical so the detailed covariance matrix was not derived.

Seven sources of random error and twelve sources of systematic error were considered in the present investigation. These are identified briefly in Table 2, and the ranges of values we estimate appear there as well. Errors and correlations for the $^{238}\text{U}(n,f)$ standard cross section should be treated separately, not as part of the present analysis. Each of the

individual cross-section ratio data points is identified by a data point number. These data points are grouped according to neutron source used in the measurements: lithium target (data points 1-18), gas target (data points 19-45). Table 3 contains explicit values for the variable error components identified in Table 2. Table 4 indicates the correlations we believe exist between the systematic errors in the same category for the various data points. No cross-category correlations are expected to exist for these data. Some additional comments are in order regarding certain of these error components: Random component R_4 for the extrapolation correction is based on the assumption that the magnitude of the error is $\sim 25\%$ of the correction. The same is true for systematic error component S_4 . The systematic error component S_{10} is derived by assuming that each of the calculated scattering correction parameters α , β , γ and ρ (see Ref. 26) has an uncertainty of $\sim 20\%$. The uncertainty in the net correction η (see Table 1) is calculated using standard error propagation techniques (see Ref. 29), assuming the partial-correction-factor errors to be uncorrelated. Typically, the uncertainty in the net scattering correction η then amounts to $\sim 30\%$ of the correction. The neutron-energy-difference dependence of the correlations for systematic error components S_8 and S_{10} , expressed in Table 4, are merely plausible assumptions reflecting the fact that neighboring-energy data points are believed to be more strongly correlated than points widely separated in energy. Systematic error component S_{12} can be calculated only if information on the cross-section excitation function shape and the energy scale uncertainty is available. Energy-scale uncertainty, as indicated previously, is assumed to be $\sim 20\%$ of the FWHM resolution. Shape sensitivity values ($\partial\sigma/\partial E$) were deduced from an eyeguide to our experimental results. Further discussion on this eyeguide appears in Section V.

IV. EXPERIMENTAL RESULTS AND DISCUSSION

The isotopic, energy-dependent $^{51}\text{V}(n,p)^{51}\text{Ti}$ cross section results from this experiment are presented in Table 5. We emphasize the experimental ratios and corresponding errors since these are obtained directly from the measurements. However, (n,p) cross sections are derived readily from these ratios by using ENDF/B-V [10] evaluated cross sections for the standard ^{238}U fast-neutron fission reaction. The overall uncertainty in a derived (n,p) cross section is obtained by combining the ratio and standard errors in quadrature. As indicated in Section III, a ratio-data covariance matrix could be calculated from information given in Tables 2-4. In order to then obtain an (n,p)-cross-section covariance matrix, this ratio covariance matrix would need to be combined with the ^{238}U fission cross section covariance matrix, deduced from the appropriate ENDF/B-V File 33 entry, using the method described in Ref. 29.

Comparisons are made between the present experimental results and experimental and evaluated values from the literature in Figs. 2 and 3. The present data span a range of more than three orders of magnitude in cross section, providing detailed definition of the threshold region for this reaction (see Fig. 2). These results cannot be readily compared with experimental values from the literature [1,31-47] since there is no over-

lap in the energy ranges. Previous experimental data correspond to the 13 to 20 MeV energy range only. Since these higher-energy results are not easily distinguished in Figs. 2 and 3, they have been plotted in Fig. 4 using a scale which exhibits greater detail. However, the present results can be readily compared with three reported evaluations, namely ENDF/B-IV and -V [10] and JENDL-2 [48]. These evaluated cross sections are for elemental vanadium, but the 0.25% difference between the elemental vanadium and ^{51}V isotopic values is generally negligible. However, the sizable differences between ENDF/B-V [10] and the present results below ~ 3 MeV can possibly be explained as follows: ENDF/B-V [10] includes the $^{50}\text{V}(n,p)^{50}\text{Ti}$ contribution to the elemental vanadium (n,p) cross section. The Q-value for $^{50}\text{V}(n,p)^{50}\text{Ti}$ is + 2.995 MeV while that for $^{51}\text{V}(n,p)^{51}\text{Ti}$ is -1.684 MeV [2]. Therefore it probably contributes in a dominant way to the elemental (n,p) cross section near threshold. Above 5 MeV, the present results also differ noticeably from the ENDF/B-V [10] evaluation. The present values are larger than the evaluated ones (by as much as 50% at ~ 8 MeV) in this energy region. The differences are even more pronounced when comparison is made to ENDF/B-IV [10]. The JENDL-2 [48] evaluation is in good agreement with our data in the 8-9 MeV range, but is not in very good agreement below ~ 7.5 MeV.

Over much of the energy range of this experiment, the errors in the measured ratios are ~ 5 -6% while the derived cross section errors are ~ 6 -7%. Near the lower-energy end, the statistical errors in measured ^{51}Ti activity and the systematic errors attributed to neutron-energy uncertainty are the dominant errors. The agreement between cross section values measured using the lithium target and those measured using the gas target is very good in the overlap region ~ 4.7 MeV, indicating that the experiment was not affected by any serious source-related systematic disturbances. It is evident from Table 5 and Figs. 2 and 3 that the outcome of tests to determine the reproducibility of several measured values was favorable.

V. INTEGRAL DIFFERENTIAL COMPARISONS

While no experimental monoenergetic data have been reported for $^{51}\text{V}(n,p)^{51}\text{Ti}$ in the energy region of interest for this experiment, some integral results have been measured and they can be indirectly compared with our results. Two standard neutron spectra commonly used to test differential data are the ^{235}U thermal-neutron-induced-fission neutron spectrum and the ^{252}Cf spontaneous-fission neutron spectrum [49]. ^{252}Cf sources can be made very compact so that only small perturbations are produced by the encapsulation material. Consequently, the spectra from such sources can be very well characterized in principle and considerable recent effort has been devoted to investigating this standard neutron field (e.g., see Refs. 50-54). A survey of CINDA [1] revealed two measured ^{252}Cf fission-spectrum-average values for the $^{51}\text{V}(n,p)^{51}\text{Ti}$ reaction [55,56]. These data are listed in Table 6. It is far more difficult to produce and characterize the standard ^{235}U thermal-neutron-induced fission neutron spectrum [57]. In reality, integral measurements have been reported for spectra ranging from those for typical fast

reactors to relatively pure ^{235}U benchmark fields. For endoergic reactions with threshold energies of a few MeV, such as $^{51}\text{V}(n,p)^{51}\text{Ti}$, the integral ratios should respond predominantly to the high-energy tails of these spectra. These tail regions differ less in shape from one facility to another than do the lower-energy portions. A survey of CINDA [1] revealed two reactor fission-spectrum average values for $^{51}\text{V}(n,p)^{51}\text{Ti}$ [58,59]. These are also listed in Table 6.

Our differential results cannot be directly compared with these integral values. However, the relationship between integral and differential cross sections is expressed by the equation

$$\langle\sigma\rangle = \int_0^{\infty} \sigma(E)\phi(E)dE / \int_0^{\infty} \phi(E)dE, \quad (1)$$

where $\langle\sigma\rangle$ is the integral value, $\sigma(E)$ is the energy-dependent cross section, and $\phi(E)$ is the neutron spectrum. Clearly, knowledge of the shape ϕ vs. energy is adequate. A normalized representation of σ vs. energy is required. These functions must be characterized over the entire response range of the integrand, $\sigma\phi$. In the present analysis, we rely on the ENDF/B-V [10] representation for the ^{235}U fission neutron spectrum. For the ^{252}Cf fission neutron spectrum we utilize a representation based on results from Refs. 50 and 51. In this work we generate $\sigma(E)$ applicable for this analysis as follows: From threshold to ~ 9.2 MeV, we rely upon an eyeguide through data points from the present experiment. In the range 9.2 - 10.5 MeV we interpolate between the curve based on our lower-energy data and the higher-energy ENDF/B-V curve. From 10.5 to 20 MeV, we accept the ENDF/B-V evaluation [10]. The resulting curve is compared with experimental data in Fig. 5. The corresponding numerical values appear in Table 7.

We have performed the calculation indicated by Eq. (1) using both of the standard fission spectra mentioned above and various $\sigma(E)$. These include the smooth curve described in the preceding paragraph and the ENDF/B-IV and-V [10] and JENDL-2 [48] evaluations for $\text{V}(n,p)\text{Ti}$. The method used in this analysis is described in Ref. 60. The calculated values are summarized in Table 6. This analytical procedure generates graphical output, which we show for the present version of $\sigma(E)$, with both the ^{235}U and ^{252}Cf fission-neutron fields, in Figs. 6 and 7, respectively. The present experimental data span $\sim 90\%$ of the ^{235}U -fission-spectrum response range, and, correspondingly, $\sim 86\%$ for ^{252}Cf . In each instance, less than 1% of the response not covered by these measurements is from the lowest energies while the rest is from above 9.3 MeV. The impact of the other reported differential data (all above ~ 13 MeV) is negligible in this context.

For the ^{235}U fission-neutron spectrum, the available measured integral values [58,59] agree fairly well with the calculation based on

ENDF/B-V [10], while the calculated integral result based on the present experimental data is noticeably larger. This discrepancy appears to exceed the indicated errors. However, the calculated integral result derived from JENDL-2 [48] agrees well with integral results calculated from the present cross sections. The ENDF/B-IV [10] $\sigma(E)$ curve yields what seems to be an unreasonably large spectrum-average cross section. For the ^{252}Cf fission neutron spectrum, one notices a discrepancy between the reported measured integral values [55,56]. We are inclined to have greater confidence in the result of Kobayashi et al. [56] since it was obtained as part of a comprehensive set of measurements involving several reactions, including the well-established standards $^{58}\text{Ni}(n,p)^{58}\text{Co}$ and $^{56}\text{Fe}(n,p)^{56}\text{Mn}$. The work of Kobayashi et al. [56] includes a detailed uncertainty analysis, and their measured integral values for the $^{58}\text{Ni}(n,p)^{58}\text{Co}$ and $^{56}\text{Fe}(n,p)^{56}\text{Mn}$ reactions, whose response profiles bracket that of $^{51}\text{V}(n,p)^{51}\text{Ti}$ in energy range, agree well with accepted values [61]. The spectrum-average value we calculate for $^{51}\text{V}(n,p)^{51}\text{Ti}$ using $\sigma(E)$ based on Table 7 agrees to within $\sim 3\%$ with the measured integral value from Kobayashi et al. [56]. The calculated result based on $\sigma(E)$ from ENDF/B-V [10] is significantly lower than the value of Kobayashi et al. [56], while use of ENDF/B-IV [10] produces a much higher result, just as it did for the ^{235}U fission neutron spectrum. For JENDL-2 [48], the agreement with the experimental data of Kobayashi et al. [56] and the present calculated results is also quite good. The fact that a favorable comparison is observed between our present results and the work of Kobayashi et al. [56] for the ^{252}Cf spectrum, while a much less favorable comparison emerges for the ^{235}U spectrum [59], is puzzling. The work of Kobayashi et al. [56,59] yields ratios of ^{252}Cf -to- ^{235}U spectrum-average cross sections of 1.41 for $^{56}\text{Fe}(n,p)^{56}\text{Mn}$ ($Z = 26$, $Q = -2.917$ MeV [2]) and 1.12 for $^{54}\text{Fe}(n,p)^{54}\text{Mn}$ ($Z = 26$, $Q = +0.088$ MeV [2]). Thus, it appears that the lower the Q -value for the reaction, the larger the corresponding observed ratio. The $^{51}\text{V}(n,p)^{51}\text{Ti}$ reaction ($Z = 23$, $Q = -1.684$ MeV [2]) offers conditions which are between the conditions for the two Fe isotopes, qualitatively, if one assumes that the somewhat lower Z value produces an effect roughly comparable to increasing the reaction Q -value for the purpose of comparison with Fe. Thus, the ^{252}Cf -to- ^{235}U spectrum average cross section ratio for $^{51}\text{V}(n,p)^{51}\text{Ti}$ of 1.56 obtained by Kobayashi et al. [56,59] seems anomalously high in this context. We deduce a corresponding ratio of 1.28 from our calculated results, which appears to be systematically more reasonable. This plausibility argument does not clearly settle the issue. There is no obvious way to establish whether the ^{252}Cf spectrum result or the ^{235}U spectrum result from the work of Kobayashi et al. [56,59] is responsible for the anomaly, assuming that one accepts the existence of an anomaly. This matter should be studied further.

VI. CONCLUSIONS

The present experiment provides cross section data of good accuracy, detail and broad energy scope, and they are relevant to established needs for applied nuclear energy programs, especially for fusion where vanadium is considered likely to be an important structural material. Comparison of the pre-

sent results with fission-spectrum integral data had an inconclusive outcome. For the ^{252}Cf spectrum the agreement between our work and the integral result believed to be the most reliable of two experimental values available from the literature is excellent ($\sim 3\%$ difference). The comparison involving the ^{235}U spectrum is much less favorable ($\sim 18\%$ difference). The origin of this discrepancy is not identified. Contemporary ^{252}Cf -spectrum measurements are considered to be more reliable, generally, than reactor-fission spectrum measurements. The principal reason for this is that reactor spectrum characterizations are more uncertain than for the ^{252}Cf spectrum. We tend to be more confident in the ^{252}Cf integral-differential comparison than in the ^{235}U comparison. This matter has to be considered as unresolved, pending further integral studies.

The results of this experiment, when compared with three independent previous evaluations, raise an issue of more general importance. The ENDF/B-IV, -V [10] and JENDL-2 [48] evaluations are all based upon independent model calculations. However, they are clearly linked by the obvious fact (see Fig. 4) that each is normalized to agree with experimental data ~ 14 MeV. It has been contended that contemporary model codes are often adequate for the task of interpolating and even extrapolating sparse nuclear data for evaluation purposes (e.g., Ref. 6). We believe that the present investigation (as is indicated clearly in Fig. 3) provides some convincing evidence to the contrary. It is apparent that when a physical quantity needs to be known to few-percent accuracies then an experimental determination is essential. Refinements in the nuclear models, and the use of model parameterizations validated by comparison with experimental data, may eventually lead to improved calculational reliability in the future. Further research directed toward achieving this objective is important for applied nuclear technology since there are reactions which are inaccessible by contemporary measurement technique, and which may, in fact, never be practical to investigate experimentally.

ACKNOWLEDGEMENTS

This work was supported by the U. S. Department of Energy. One of the authors (I.K.) gratefully acknowledges support provided by the American Nuclear Society International Student Exchange Program. The authors are indebted to Dr. K. Kobayashi from the Kyoto University Research Reactor Institute for his valuable assistance with this work.

REFERENCES

1. CINDA-A (1935-1976) Vol. I- June 1979; CINDA-83 (1977-1983)- May 1983: "An Index to the Literature on Microscopic Neutron Data," International Atomic Energy Agency, Vienna, Austria.
2. Table of the Isotopes, 7th Edition, C. Michael Lederer and Virginia S. Shirley, Eds., John Wiley and Sons, Inc., New York (1978).
3. E. T. Cheng, D. R. Mathews and K. K. Schultz, "Magnetic Fusion Energy Program Nuclear Data Needs," GA-A16886, General Atomic Company, P. O. Box 81608, San Diego, California 92138 (1982).
4. "Compilation of Requests for Nuclear Data," compiled and edited by the National Data Center for the DOE Nuclear Data Committee, BNL-NCS-51572, Brookhaven National Laboratory, Upton, New York 11973 (1983).
5. Donald L. Smith, "Neutron Dosimetry for Radiation Damage in Fission and Fusion Reactors," in "Proceedings of an International Conference on Nuclear Cross Sections for Technology," University of Tennessee, Knoxville, Tennessee, October 22-26, 1979, Eds. J. L. Fowler and C. H. Johnson, NBS Special Publication 594, National Bureau of Standards, U.S. Department of Commerce, Washington, D.C., p. 285 (1980).
6. Robert C. Haight, "Applied Uses of Nuclear Level Densities," in "Proceedings of an Advisory Group Meeting on Basic and Applied Problems of Nuclear Level Densities," Brookhaven National Laboratory, April 11-15, 1983, Ed. M. Bhat, BNL-NCS-51694, National Nuclear Data Center, Brookhaven National Laboratory, Upton, New York 11973 (1983).
7. A. Paulsen, H. Liskien, F. Arnotte and R. Widera, Nucl. Sci. Eng. 78, 377 (1981).
8. H. Liskien and A. Paulsen, Annals of Nuclear Energy 8, 423 (1981).
9. S. M. Grimes, R. C. Haight, K. K. Alvar, H. H. Barschall and R. R. Borchers, Phys. Rev. C19, 2127 (1979).
10. "Evaluated Neutron Data File, ENDF/B", National Nuclear Data Center, Brookhaven National Laboratory, Upton, New York 11973. Reference is made in the present work to both the ENDF/B-IV and -V versions of this file.
11. James W. Meadows and Donald L. Smith, "Neutron Source Investigations in Support of the Cross Section Program at the Argonne Fast-Neutron Generator," ANL/NDM-53, Argonne National Laboratory, Argonne, Illinois 60439 (1980).

12. S. A. Cox and P. R. Hanley, IEEE Trans. Nucl. Sci. 18, 108 (1971).
13. J. W. Meadows and D. L. Smith, "Neutrons from Proton Bombardment of Natural Lithium," ANL-7938, Argonne National Laboratory, Argonne, Illinois 60439 (1972).
14. Horst Liskien and Arno Paulsen, Atomic Data and Nuclear Data Tables 15, 57 (1975).
15. D. L. Smith and J. W. Meadows, "Method of Neutron Activation Cross Section Measurement for $E_n = 5.5 - 10$ MeV Using the $D(d,n)He-3$ Reaction as a Neutron Source," ANL/NDM-9, Argonne National Laboratory, Argonne, Illinois 60439 (1974).
16. James W. Meadows, Donald L. Smith and Gerhard Winkler, Nucl. Instr. and Meth. 176, 439 (1980).
17. Donald L. Smith, "Some Comments on Resolution and the Analysis and Interpretation of Experimental Results from Differential Neutron Measurements," ANL/NDM-49, Argonne National Laboratory, Argonne, Illinois 60439 (1979).
18. Donald L. Smith, "A Least-Squares Method for Deriving Reaction Differential Cross Section Information from Measurements Performed in Diverse Neutron Fields," ANL/NDM-77, Argonne National Laboratory, Argonne, Illinois 60439 (1982).
19. E. H. Beckner, R. L. Bramblett, G. C. Phillips and T. A. Eastwood, Phys. Rev. 123, 2100 (1961).
20. J. B. Marion, Rev. Mod. Phys. 38, 660 (1966).
21. J. W. Meadows, Nucl. Sci. Eng. 49, 310 (1972).
22. Donald L. Smith and James W. Meadows, "Response of Several Threshold Reactions in Reference Fission Neutron Fields," ANL/NDM-13, Argonne National Laboratory, Argonne, Illinois 60439 (1975).
23. W. P. Poenitz, J. W. Meadows and R. J. Armani, " ^{235}U Fission Mass and Counting Comparison and Standardization," ANL/NDM-48, Argonne National Laboratory, Argonne, Illinois 60439 (1979).
24. Standard ^{152}Eu Gamma Calibration Source, Type EGMA3, No. 5243, Laboratoires de Metrologie des Rayonnements Ionisants, Commissariat a l'Energie Atomique, Saclay, BP No. 2, 91190 Gif sur Yvette, France.
25. Mixed-Radionuclide Point-Source Standard, No. SRM 4275-140, National Bureau of Standards, Washington, D.C. 20234, U.S.A.

26. Donald L. Smith and James W. Meadows, "Measurement of $^{58}\text{Ni}(n,p)^{58}\text{Co}$ Reaction Cross Sections for $E_n=0.44-5.87$ MeV Using Activation Methods," ANL-7989, Argonne National Laboratory, Argonne, Illinois 60439 (1973).
27. J. E. Simons and R. L. Henkel, Phys. Rev. 120, 198 (1960).
28. D. L. Smith and J. W. Meadows, "Neutron Inelastic Scattering Studies for Lead-204," ANL/NDM-37, Argonne National Laboratory, Argonne, Illinois 60439 (1977).
29. Donald L. Smith, "Covariance Matrices and Applications to the Field of Nuclear Data," ANL/NDM-62, Argonne National Laboratory, Argonne, Illinois 60439 (1981).
30. Donald L. Smith, "Non-Evaluation Applications for Covariance Matrices," ANL/NDM-67, Argonne National Laboratory, Argonne, Illinois 60439 (1982).
31. N. I. Molla and S. M. Qaim, Nucl. Phys, A283, 269 (1977).
32. D. Crumpton, J. Inorg. Nucl. Chem. 31, 3727 (1969).
33. B. Mitra and A. M. Ghose, Nucl. Phys. 83, 157 (1966).
34. J. C. Robertson, B. Audric and P. Kolkowski, Journal of Nuclear Energy 27, 531 (1973).
35. W. H. Warren and W. L. Alford, Ann. Nucl. Energy 9, 369 (1982).
36. E. T. Bramlitt and R. W. Fink, Phys. Rev. 131, 2649 (1963).
37. Schwerer et al., Oesterr. Akad. Wiss., Math. + Naturw. Anzeiger 113, No. 9, 153 (1976). Data obtained from Computer Files on Microscopic Neutron Data, EXFOR 20811.004, International Atomic Energy Agency, Vienna.
38. M. Borman, S. Cierjacks, R. Langkau and H. Neuert, Zeit. Physik 166, 477 (1962).
39. Dresler et al., INR-1464, 12, Inst. Badan Jadrowych (Nucl. Res.), Warsaw, Poland. Data obtained from Computer Files on Microscopic Neutron Data, EXFOR 30263.006, International Atomic Energy Agency, Vienna.
40. R. Prasad and D. C. Sarkar, Nuovo Cimento 3A, 467 (1971).
41. Tikku et al., Nucl. Phys. & Solid State Phys. Sympos., Chandigarh, India, Jan. 1973, Vol. 2, Nucl. Phys. Data obtained from Computer Files on Microscopic Neutron Data, EXFOR 30394.004, International Atomic Energy Agency, Vienna.

42. Deak et al., Second International Symposium on Neutron Induced Reactions, Smolenice, Czechoslovakia, 25-29 June 1979. Data obtained from Computer Files on Microscopic Neutron Data, EXFOR 30562.008, International Atomic Energy Agency, Vienna.
43. V. N. Levkovskii, Sov. J. Nucl. Phys. 18, 361 (1973).
44. C. S. Khurana and I. M. Govil, Nucl. Phys. 69, 153 (1965).
45. J. E. Strain and W. J. Ross, "14-MeV Neutron Reactions," ORNL-3672, Oak Ridge National Laboratory, Oak Ridge, Tennessee (1965).
46. E. B. Paul and R. L. Clarke, Can. J. Phys. 31, 267 (1953).
47. A. Poularikas, A-ARK-60, 3, Univ. of Arkansas, (1960). Data obtained from Computer Files on Microscopic Neutron Data, EXFOR 11683.003, International Atomic Energy Agency, Vienna.
48. Shigeya Tanaka, "Evaluation of Neutron Cross Sections for Vanadium," JAERI-M-82-151, Japan Atomic Energy Research Institute, Tokai-mura, Naka-gun, Ibaraki-ken 319-11, Japan.
49. H. H. Knitter, "A Review on Standard Fission Neutron Spectra of ^{235}U and ^{252}Cf ," Neutron Cross Sections for Reactor Dosimetry, Review Papers, Vol. 1, Proceedings of a Consultant's Meeting on Integral Cross-section Measurements in Standard Neutron Fields for Reactor Dosimetry, Ed. M. Vlasov, IAEA-208, International Atomic Energy Agency, Vienna, p. 183 (1978).
50. W. P. Poenitz and T. Tamura, "Investigation of the Prompt-Neutron Spectrum for Spontaneously-Fissioning ^{252}Cf ," Nuclear Data for Science and Technology, Proceedings of an International Conference, Antwerp, Belgium, 6-10 September 1982, Ed. K. H. Boeckhoff, D. Reidel Publishing Company, Dordrecht, Netherlands, p. 465 (1983).
51. D. G. Madland and J. R. Nix, "Calculation of the Prompt Neutron Spectrum and Average Prompt Neutron Multiplicity for the Spontaneous Fission of ^{252}Cf ," *ibid.* Ref. 50, p. 473.
52. M. V. Blinov, G. S. Boykov and V. A. Vitenko, "New Experimental Data on the Energy Spectrum of ^{252}Cf Spontaneous Fission Prompt Neutrons," *ibid.* Ref. 50, p. 479.
53. R. Boettger, H. Klein, A. Chalupka and B. Strohmaier, "The Neutron Energy Spectrum from the Spontaneous Fission of ^{252}Cf in the Energy Range $2 \text{ MeV} \leq E_n \leq 14 \text{ MeV}$," *ibid.* Ref. 50, p. 484.
54. H. Maerten, D. Seeliger and B. Stobinski, "The High-Energetic Part of the Neutron Spectrum from Spontaneous Fission of ^{252}Cf ," *ibid.* Ref. 50, p. 488.

55. Z. Dezso and J. Csikai, "(n,p) and (n,f) Cross Section Measurements for ^{252}Cf Neutron Spectrum," ZFK-376, 44, Zentralinst. f. Kernforschung, Rossendorf, D. R. Germany (1978).
56. Katsuhei Kobayashi, Itsuro Kimura and Wolf Mannhart, "Measurement and Covariance Analysis of Californium-252 Spectrum-Averaged Cross Sections," J. Nuclear Science and Technology 19, p. 341 (1982).
57. J. Grundl and C. Eisenhauer, "Benchmark Neutron Fields for Reactor Dosimetry," Neutron Cross Sections for Reactor Dosimetry, Review Papers, Vol. 1, Proceedings of a Consultant's Meeting on Integral Cross-section Measurements in Standard Neutron Fields for Reactor Dosimetry, Ed. M. Vlasov, IAEA-208, International Atomic Energy Agency, Vienna, p. 53 (1978).
58. F. Nasyrov, Soviet Atomic Energy 25, 1251 (1968).
59. Katsuhei Kobayashi, Itsuro Kimura, Masaharu Nakazawa and Masatsugu Akiyama, J. Nuclear Science and Technology 13, 531 (1976).
60. Donald L. Smith, "Analysis of the Sensitivity of Spectrum-Average Cross Sections to Individual Characteristics of Differential Excitation Functions," ANL/NDM-30, Argonne National Laboratory, Argonne, Illinois 60439 (1977).
61. Benjamin A. Magurno, "ENDF/B-V Data Testing Report, Contribution by the Special Application File Subcommittee (SAFE), Cross Section Evaluation Working Group (CSEWG)," unpublished report, National Nuclear Data Center, Brookhaven National Laboratory, Upton, New York 11973 (1982).

Table 1: Calculated Neutron Multiple Scattering Correction Parameters^a

E_n (MeV)	α	β	γ	ρ	<u>Net Correction η^b</u>
2.0	0.0	0.0	7.5 ^c	4.2 ^c	11.7 ^c
3.0	5.0	1.4	7.7	4.4	5.7
3.331	3.5	0.9	7.8	4.1	7.5
4.139	4.1	0.8	7.7	3.8	6.6
4.336	4.2	1.0	7.8	4.2	6.8
5.039	3.8	1.0	7.5	4.2	6.9
5.240	3.6	0.8	7.8	3.5	6.9
6.268	3.7	0.5	7.1	3.3	6.2
7.264	3.3	0.5	6.5	2.9	5.6
8.242	3.0	0.5	6.4	2.3	5.2
9.210	2.7	0.5	6.0	2.2	5.0
10.17	2.7	0.5	5.8	2.0	4.6

^a Parameters are as defined in Ref. 26. All values are given in percent.

^b $\eta = \text{Abs}[(\alpha + \beta) - (\gamma + \rho)]$.

^c Estimated values.

Table 2: Sources of Experimental Error

RANDOM ERRORS		
<u>Symbol</u>	<u>Magnitude (%)</u>	<u>Description</u>
R ₁	0.2	Exposure, waiting and counting times.
R ₂	0.3 - 47.8	0.320-MeV gamma-ray yield.
R ₃	0.7 - 1.5	Fission yield.
R ₄	1 - 2	Extrapolation correction.
R ₅	N - 3 ^a	Background fission correction.
R ₆	0.2 - 1.2	Background activation.
R ₇	1.5	Geometric corrections.

SYSTEMATIC ERRORS		
<u>Symbol</u>	<u>Magnitude (%)</u>	<u>Description</u>
S ₁	0.1	⁵¹ Ti decay half life.
S ₂	2	²³⁸ U content of monitor deposit.
S ₃	0.2	⁵¹ V content of samples.
S ₄	0.8	Uranium deposit thickness correction.
S ₅	2.4	Gamma-ray counting efficiency.
S ₆	1	⁵¹ Ti gamma-ray decay branch factor.
S ₇	N ^a	Orientation of sample for counting.
S ₈	2	Neutron source properties.
S ₉	N ^a	Room-return fission events.
S ₁₀	1.4 - 2.1	Neutron scattering corrections.
S ₁₁	1.5	Geometric corrections.
S ₁₂	0.5 - 19.5	Average neutron energy.

^a N = Negligible

Table 3: Explicit Values for Variable Error Components^a (Continued)

<u>Data Point^b</u>	<u>R₂</u>	<u>R₃</u>	<u>R₄</u>	<u>R₅</u>	<u>R₆</u>	<u>S₁₀</u>	<u>S₁₂</u>
43	0.3	0.8	1.0	2.5	1.0	1.4	1.0
44	0.3	0.9	1.0	3.0	1.0	1.4	1.1
45	0.3	0.9	1.0	3.0	1.2	1.4	1.1

^a Values in percent. See Table 2 for error component descriptions.

^b Neutron source: Lithium target (Data Points 1-18). Gas target (Data Points 19-45).

^c N=Negligible.

Table 4: Systematic Error Component Correlations

<u>Symbol</u>	<u>Assumed Correlations (%)</u>
S ₁	100
S ₂	100
S ₃	100
S ₄	100
S ₅	100
S ₆	100
S ₇	Not applicable ^a
S ₈	No correlation between lithium and gas target points. Otherwise (100-10ΔE) ^b
S ₉	Not applicable ^a
S ₁₀	(100-10ΔE) ^b
S ₁₁	100
S ₁₂	100

^a Error component is negligible.

^b ΔE is the magnitude of the difference in the neutron energies for the two data points, in MeV.

Table 5: $^{51}\text{V}(n,p)^{51}\text{Ti}$ Reaction Cross-Section Results

Data ^a Point	E_n (MeV)	Resolution ^b (MeV)	Measured Ratio	Ratio Random Error(%)	Ratio Systematic Error(%)	Ratio Total Error(%)	$\sigma_{F,238}^c$ (mb)	Error ^c in $\sigma_{F,238}$ (%)	σ_{np} (mb)	Error in σ_{np} (%)
1	2.856	0.095	9.075(-6) ^d	47.9	15.6	50.4	528.8	3.0	0.004799	50.5
2	2.957	0.094	1.966(-5)	20.6	9.2	22.6	524.4	3.0	0.01031	22.8
3	3.057	0.094	2.575(-5)	15.9	20.1	25.6	522.7	2.5	0.01346	25.7
4	3.158	0.092	7.369(-5)	6.7	15.5	16.9	524.2	2.5	0.03863	17.1
5	3.258	0.090	1.441(-4)	4.9	11.2	12.2	526.7	2.5	0.07588	12.5
6	3.359	0.087	2.354(-4)	3.6	8.1	8.9	529.2	2.5	0.1246	9.2
7	3.459	0.087	3.210(-4)	3.4	6.7	7.5	531.7	2.5	0.1707	7.9
8	3.560	0.087	4.130(-4)	3.2	7.8	8.4	536.1	2.5	0.2214	8.8
9	3.661	0.087	6.140(-4)	3.0	7.2	7.8	541.7	2.5	0.3326	8.2
10	3.761	0.082	7.917(-4)	2.9	8.4	8.9	544.3	2.5	0.4309	9.2
11	3.861	0.084	1.281(-3)	2.8	5.9	6.5	544.9	2.5	0.6979	7.0
12	3.861	0.084	1.282(-3)	2.8	5.9	6.5	544.9	2.5	0.6986	7.0
13	3.962	0.081	1.348(-3)	2.8	4.9	5.6	545.5	2.5	0.7353	6.1
14	4.063	0.081	1.552(-3)	2.8	5.1	5.8	546.3	2.4	0.8476	6.3
15	4.264	0.075	1.967(-3)	2.7	6.7	7.2	547.4	2.4	1.077	7.6
16	4.464	0.076	2.692(-3)	2.7	5.2	5.9	549.0	2.4	1.478	6.4

Table 5: $^{51}\text{V}(n,p)^{51}\text{Ti}$ Reaction Cross-Section Results (Continued)

Data ^a Point	E_n (MeV)	Resolution ^b (MeV)	Measured Ratio	Ratio Random Error(%)	Ratio Systematic Error(%)	Ratio Total Error(%)	$\sigma_{F,238}^c$ (mb)	Error ^c in $\sigma_{F,238}$ (%)	σ_{np} (mb)	Error in σ_{np} (%)
17	4.664	0.076	4.136(-3)	2.8	4.7	5.5	544.0	2.4	2.250	6.0
18	4.865	0.076	4.996(-3)	2.8	4.8	5.6	537.6	2.4	2.686	6.1
19	4.643	0.276	4.105(-3)	2.7	5.1	5.8	544.7	2.4	2.236	6.3
20	4.893	0.248	5.315(-3)	2.6	6.2	6.7	536.8	2.4	2.853	7.1
21	5.139	0.211	6.049(-3)	2.4	5.2	5.7	537.3	2.6	3.250	6.3
22	5.374	0.194	6.696(-3)	2.4	5.0	5.5	543.9	2.6	3.642	6.1
23	5.600	0.180	7.571(-3)	2.4	5.6	6.1	560.4	2.6	4.243	6.6
24	5.819	0.174	8.559(-3)	2.4	5.3	5.8	589.0	2.6	5.041	6.4
25	5.822	0.167	8.870(-3)	2.5	5.2	5.8	589.4	2.6	5.228	6.4
26	6.040	0.162	9.600(-3)	2.3	4.9	5.4	627.4	3.9	6.023	6.7
27	6.254	0.153	1.006 (-2)	2.3	4.8	5.3	710.0	3.9	7.142	6.6
28	6.465	0.146	9.435(-3)	2.3	4.7	5.2	796.7	3.9	7.517	6.5
29	6.675	0.149	9.317(-3)	2.3	4.7	5.2	860.0	3.9	8.013	6.5
30	6.881	0.144	1.003 (-2)	2.3	4.6	5.1	904.9	3.9	9.077	6.4
31	6.882	0.141	9.969(-3)	2.3	4.6	5.1	905.1	3.9	9.023	6.4
32	7.087	0.141	1.003(-2)	2.3	4.6	5.1	933.2	3.9	9.362	6.4

Table 5: $^{51}\text{V}(n,p)^{51}\text{Ti}$ Reaction Cross-Section Results (Continued)

Data ^a Point	E_n (MeV)	Resolution ^b (MeV)	Measured Ratio	Ratio Random Error(%)	Ratio Systematic Error(%)	Ratio Total Error(%)	$\sigma_{F,238}^c$ (mb)	Error ^c in $\sigma_{F,238}$ (%)	σ_{np} (mb)	Error in σ_{np} (%)
33	7.290	0.144	1.089(-2)	2.3	4.6	5.1	959.7	3.9	10.45	6.4
34	7.494	0.144	1.182(-2)	2.6	4.6	5.3	986.3	3.9	11.66	6.6
35	7.694	0.152	1.189(-2)	2.5	4.6	5.2	988.6	3.9	11.72	6.5
36	7.893	0.155	1.285(-2)	2.9	4.6	5.4	990.1	3.9	12.72	6.7
37	7.893	0.156	1.337(-2)	2.9	4.6	5.4	990.1	3.9	13.24	6.7
38	8.092	0.161	1.331(-2)	2.9	4.6	5.4	991.7	2.9	13.20	6.1
39	8.290	0.169	1.403(-2)	2.9	4.6	5.4	993.1	2.9	13.93	6.1
40	8.486	0.173	1.452(-2)	3.3	4.5	5.6	994.6	2.9	14.44	6.3
41	8.683	0.181	1.571(-2)	3.3	4.6	5.7	996.0	2.9	15.65	6.4
42	8.684	0.179	1.578(-2)	3.3	4.5	5.6	996.0	2.9	15.72	6.3
43	8.879	0.184	1.598(-2)	3.4	4.5	5.6	997.5	2.9	15.94	6.3
44	9.071	0.189	1.778(-2)	3.8	4.6	6.0	997.3	2.9	17.73	6.7
45	9.267	0.195	1.850(-2)	3.8	4.6	6.0	994.0	2.9	18.39	6.7

^a Neutron source: Lithium target (Data Points 1-18).
Gas target (Data Points 19-45).

^b FWHM of incident neutron distribution.

^c ^{238}U neutron fission cross section, ENDF/B-V [10].

^d 9.075(-6) signifies 9.075×10^{-6} .

Table 6: Measured and Calculated Fission-Spectrum-Average
Cross Sections for $^{51}\text{V}(n,p)^{51}\text{Ti}$

^{235}U Spectrum [10]:

<u>Origin</u>	<u>$\langle\sigma\rangle$ (mb)</u>
Integral experiment: Nasyrov [58]	0.41 ± 0.04 ^a
Integral experiment: Kobayashi et al. [59]	0.456 ± 0.023 ^a
Calculation: ENDF/B-IV $\sigma(E)$ [10]	0.9513
Calculation: ENDF/B-V $\sigma(E)$ [10]	0.4303
Calculation: JENDL-2 $\sigma(E)$ [48]	0.5146
Calculation: $\sigma(E)$ based mainly on results from present experiment (see Table 7).	0.5366

^{252}Cf Spectrum [50,51]:

<u>Origin</u>	<u>$\langle\sigma\rangle$ (mb)</u>
Integral experiment: Dezso et al. [55]	0.93 ± 0.10 ^a
Integral experiment: Kobayashi et al. [56]	0.71 ± 0.06 ^a
Calculation: ENDF/B-IV $\sigma(E)$ [10]	1.210
Calculation: ENDF/B-V $\sigma(E)$ [10]	0.5522
Calculation: JENDL-2 $\sigma(E)$ [48]	0.6466
Calculation: $\sigma(E)$ based mainly on results from present experiment (see Table 7)	0.6878

^aValues as quoted in original papers.

Table 7: Representation of $\sigma(E)$ for $^{51}\text{V}(n,p)^{51}\text{Ti}$ Based on Consideration of the Present Experimental Data and Previous Evaluations.^a

<u>E</u> (MeV)	<u>$\sigma(E)$</u> (mb)	<u>E</u> (MeV)	<u>$\sigma(E)$</u> (mb)
2.85	0.0049	6.0	6.0
2.95	0.009	7.0	9.4
3.05	0.0134	8.0	13.1
3.15	0.037	8.5	14.9
3.25	0.07	9.0	17.2
3.35	0.12	10.0	22.2
3.45	0.165	10.5	24.3
3.55	0.215	11.0	27.8
3.65	0.31	11.5	30.5
3.75	0.42	12.0	32.8
3.84	0.62	12.5	34.5
3.9	0.7	13.0	35.6
4.0	0.78	14.0	36.7
4.3	1.16	15.0	35.8
4.6	2.1	16.0	34.2
4.75	2.53	18.0	29.0
5.0	3.1	20.0	25.0
5.5	4.05		

^a See Section V of the text.

FIGURE CAPTIONS

- Fig. 1. Schematic diagram of irradiation setup for the present experiment. The gas target assembly used for ${}^2\text{H}(d,n){}^3\text{He}$ neutron production is shown.
- Fig. 2. Cross sections for the ${}^{51}\text{V}(n,p){}^{51}\text{Ti}$ reaction. Data points: Present work (O), Ref. 31 (◻), Ref. 32 (□), Ref. 33 (◇), Ref. 34 (△), Ref. 35 (⊗), Ref. 36 (⊗), Ref. 37 (●), Ref. 38 (■), Ref. 39 (◆), Ref. 40 (▲), Ref. 41 (⊗), Ref. 42 (⊗), Ref. 43 (L), Ref. 44 (K), Ref. 45 (S), Ref. 46 (E), Ref. 47 (P). Evaluation: ENDF/B-V (Ref. 10) is the solid curve. Values near 14 MeV can be seen more clearly in Fig. 4.
- Fig. 3. Cross sections for the ${}^{51}\text{V}(n,p){}^{51}\text{Ti}$ reaction. Data points: Present work (O), Ref. 31 (◻), Ref. 32 (□), Ref. 33 (◇), Ref. 34 (△), Ref. 35 (⊗), Ref. 36 (⊗), Ref. 37 (●), Ref. 38 (■), Ref. 39 (◆), Ref. 40 (▲), Ref. 41 (⊗), Ref. 42 (⊗), Ref. 43 (L), Ref. 44 (K), Ref. 45 (S), Ref. 46 (E), Ref. 47 (P). Evaluations: ENDF/B-IV (A)-Ref. 10, ENDF/B-V (B)-Ref. 10, JENDL-2 (C) - Ref. 48. Values in the threshold region are shown more clearly in Fig. 2. Values near 14 MeV can be seen more clearly in Fig. 4.
- Fig. 4. High-energy cross sections for the ${}^{51}\text{V}(n,p){}^{51}\text{Ti}$ reaction. Data points: Ref. 31 (◻), Ref. 32 (□), Ref. 33 (◇), Ref. 34 (△), Ref. 35 (⊗), Ref. 36 (⊗), Ref. 37 (●), Ref. 38 (■), Ref. 39 (◆), Ref. 40 (▲), Ref. 41 (⊗), Ref. 42 (⊗), Ref. 43 (L), Ref. 44 (K), Ref. 45 (S), Ref. 46 (E), Ref. 47 (P). Evaluations: ENDF/B-IV (A)-Ref. 10, ENDF/B-V (B) - Ref. 10, JENDL-2 (C) - Ref. 48.
- Fig. 5. Cross sections for the ${}^{51}\text{V}(n,p){}^{51}\text{Ti}$ reaction. Data points: Present work (O), Ref. 31 (◻), Ref. 32 (□), Ref. 33 (◇), Ref. 34 (△), Ref. 35 (⊗), Ref. 36 (⊗), Ref. 37 (●), Ref. 38 (■), Ref. 39 (◆), Ref. 40 (▲), Ref. 41 (⊗), Ref. 42 (⊗), Ref. 43 (L), Ref. 44 (K), Ref. 45 (S), Ref. 46 (E), Ref. 47 (P). Solid curve is based on an eyeguide to the present data and portions of previous evaluations (see Section V of text). This curve is used to calculate spectrum-average cross sections.
- Fig. 6. ${}^{235}\text{U}$ fission spectrum response analysis for ${}^{51}\text{V}(n,p){}^{51}\text{Ti}$. The cross section is based on the present work (Fig. 5 and Table 7). The neutron spectrum is the standard ${}^{235}\text{U}$ thermal-neutron-induced-fission neutron spectrum from ENDF/B-V [10]. Shown are plots of SIG - $\sigma(E)$, PHI - $\phi(E)$, SIG*PHI - $\sigma(E)\phi(E)$, and SIGP*PHI - $\partial\sigma/\partial E(E)\phi(E)$. The plot of SIG*PHI indicates the response energy range while that for SIGP*PHI shows the region of greatest energy scale sensitivity for the reaction.

Fig. 7. ^{252}Cf -fission-spectrum response analysis for $^{51}\text{V}(\text{L.P.})^{51}\text{Ti}$. The cross section is based on the present work (Fig. 5 and Table 7). The neutron spectrum is the standard ^{252}Cf spontaneous-fission neutron spectrum (e.g., Refs. 50,51). Shown are plots of $\text{SIG}-\sigma(E)$, $\text{PHI}-\phi(E)$, $\text{SIG*PHI}-\sigma(E)\phi(E)$, and $\text{SIGP*PHI}-\partial\sigma/\partial E(E)\phi(E)$. The plot of SIG*PHI indicates the response energy range while that for SIGP*PHI shows the region of greatest energy scale sensitivity for the reaction.

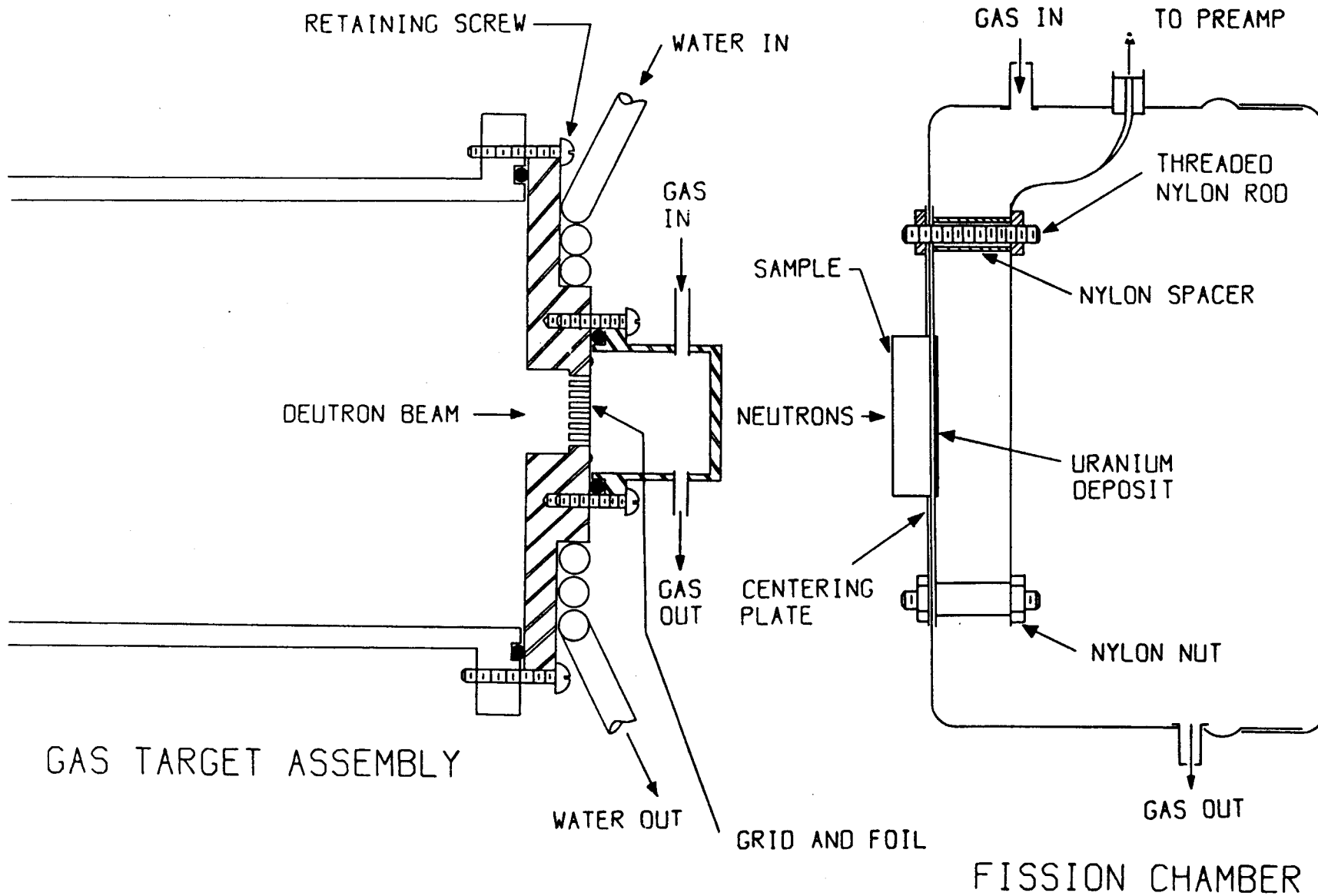


Figure 1.

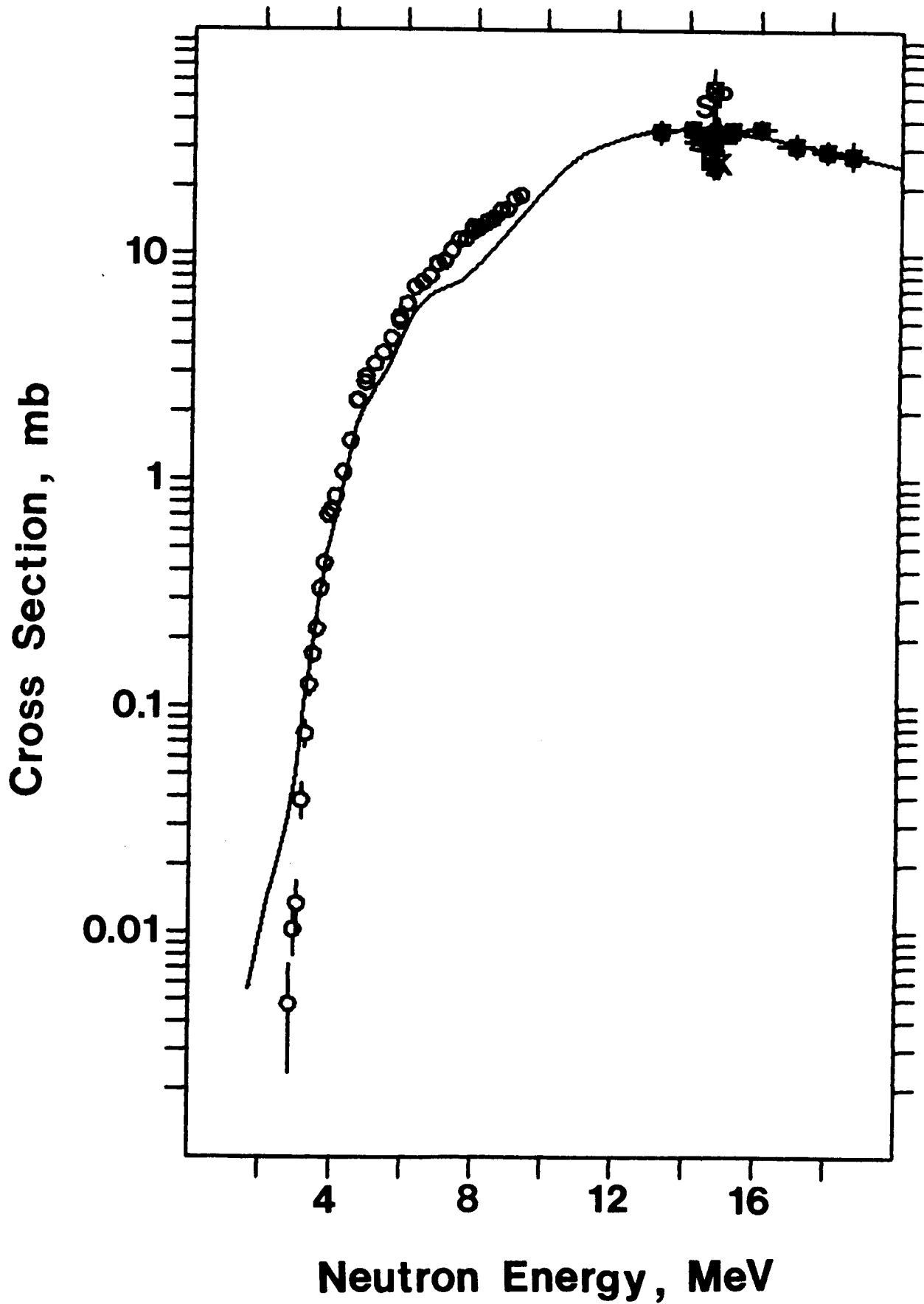


Figure 2.

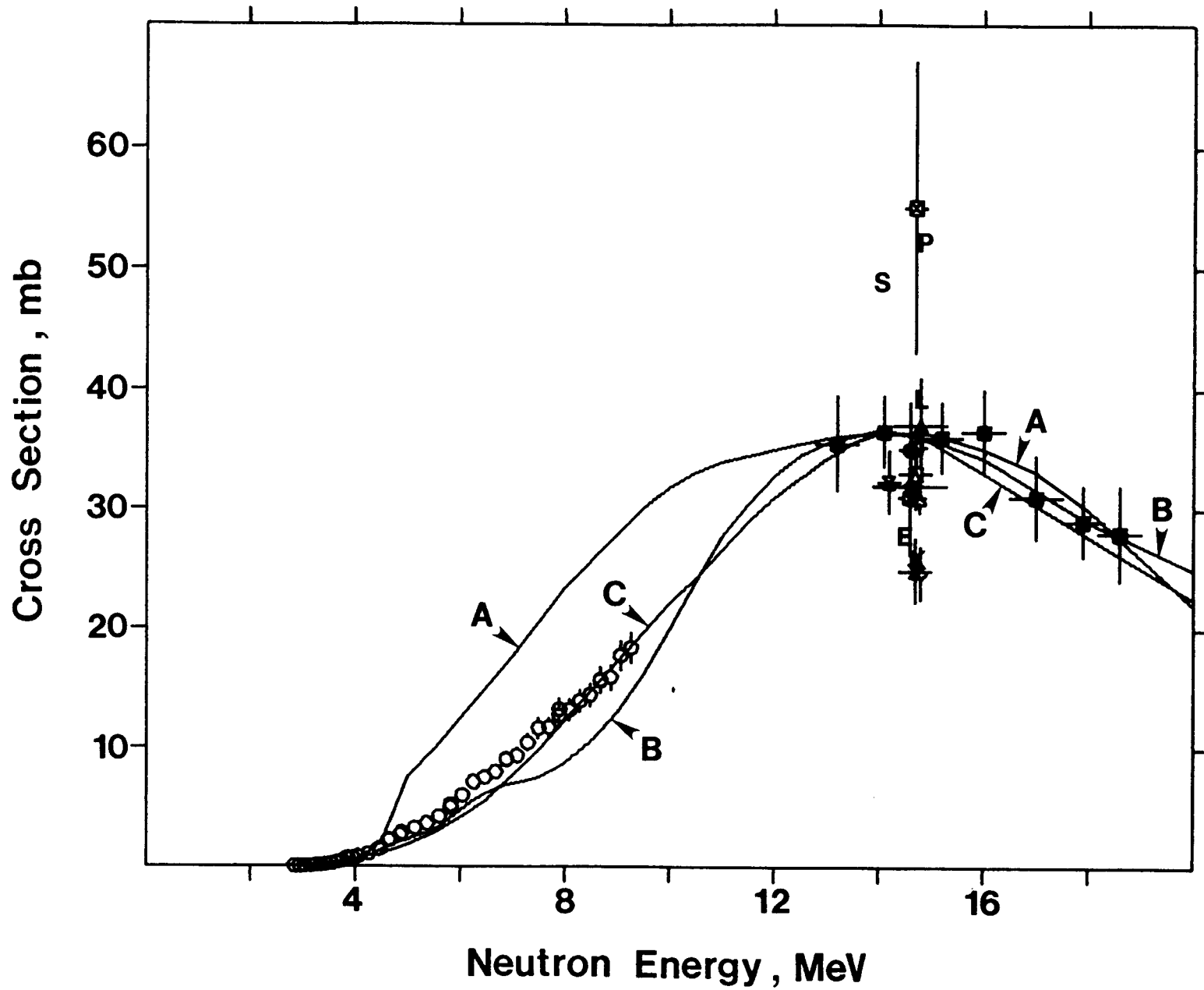


Figure 3.

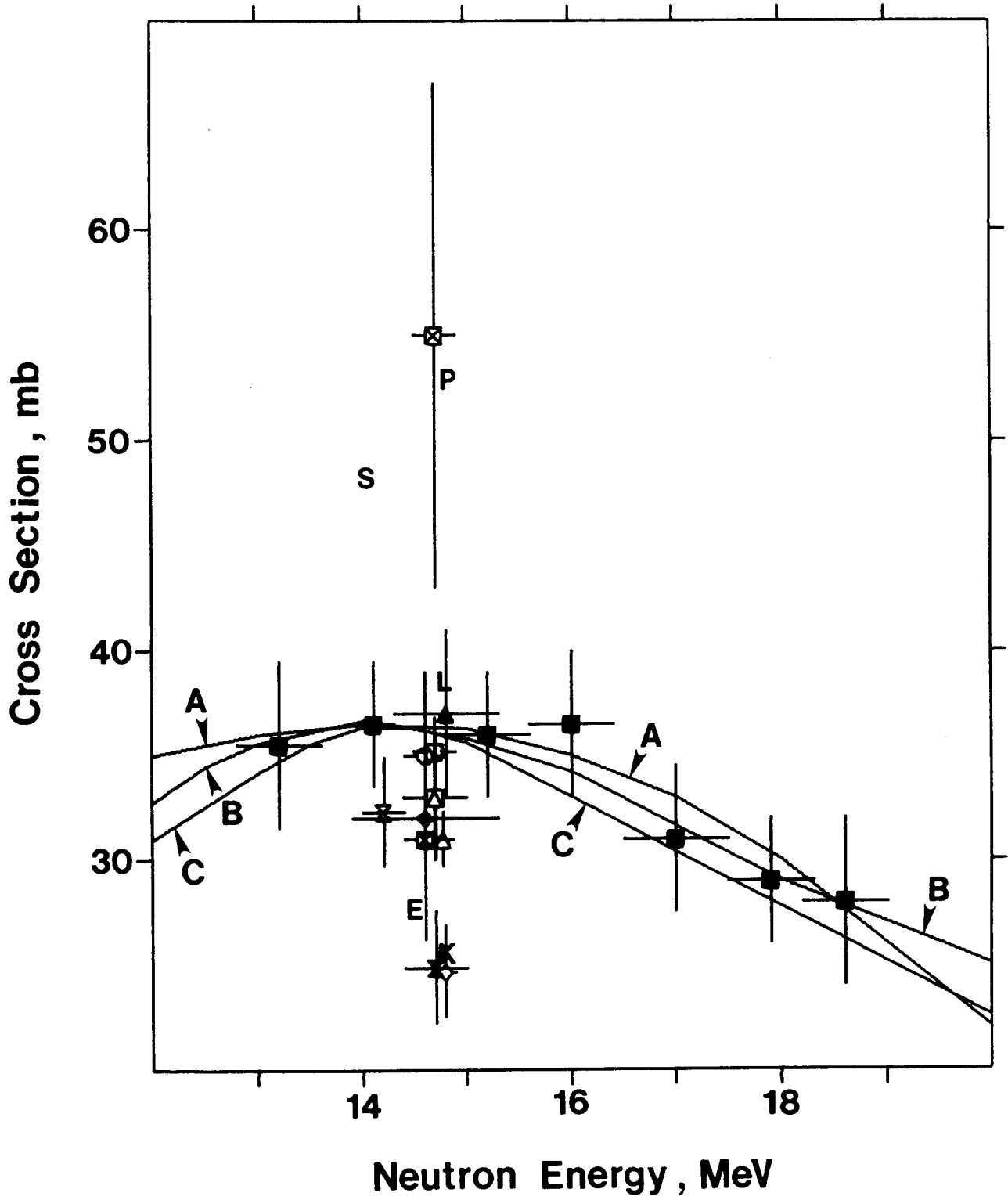


Figure 4.

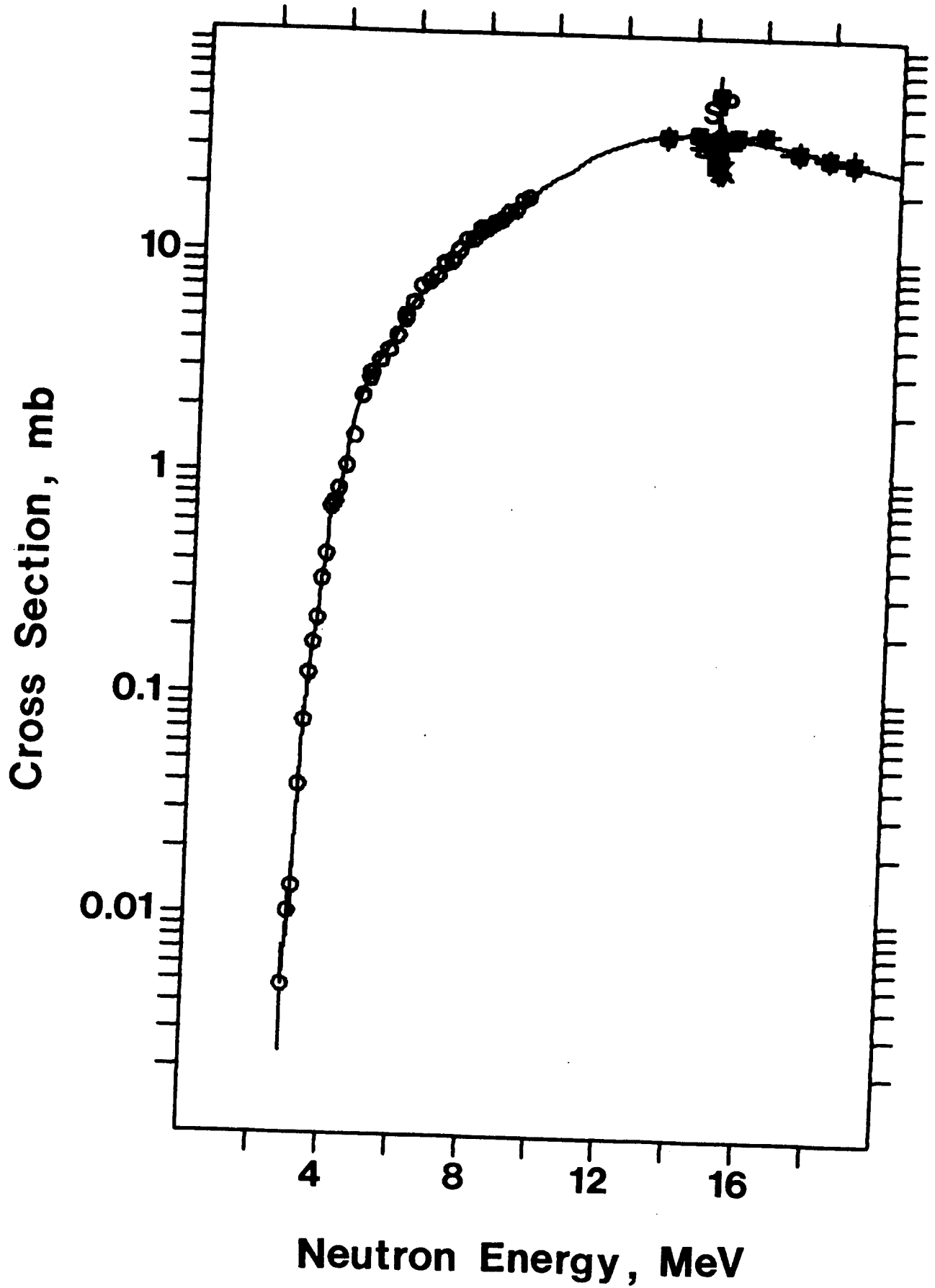
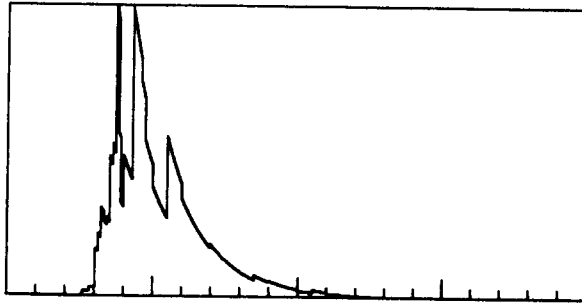
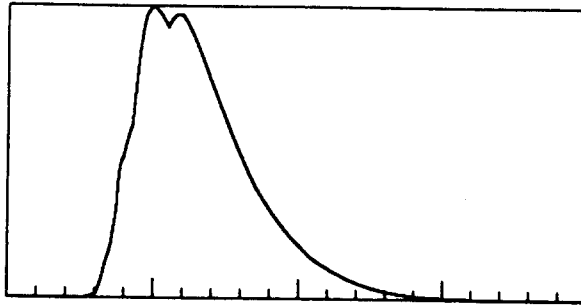


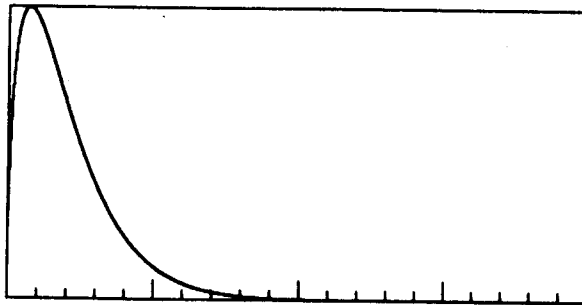
Figure 5.



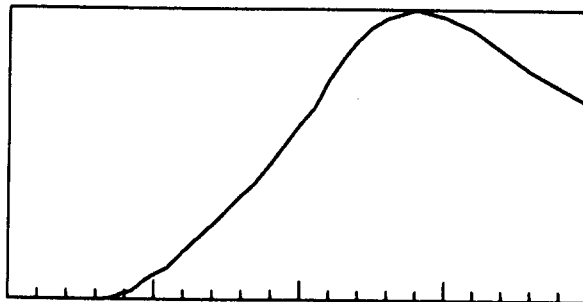
SIG*PHI



SIG*PHI



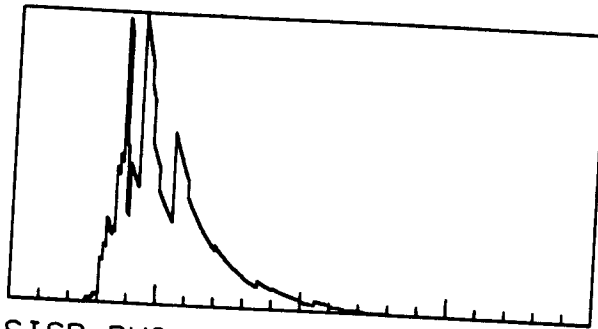
PHI



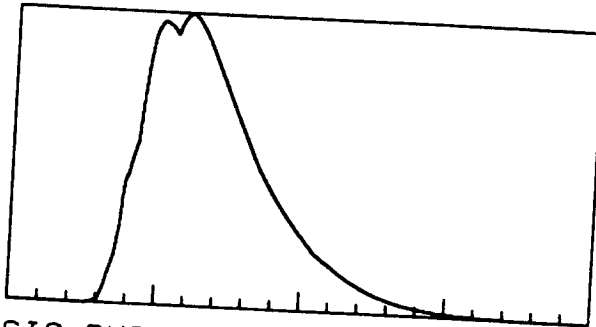
SIG

TH U5 FISSION WATTS V
V-51(N,P)TI-51 PRESENT WORK

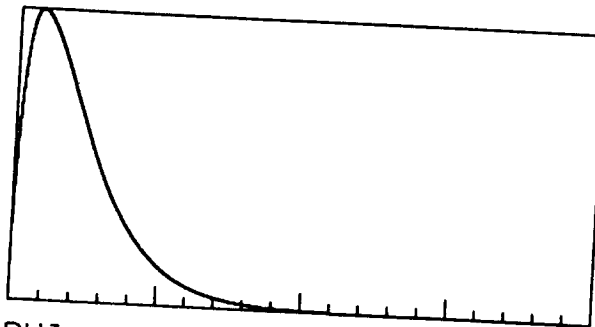
Figure 5.



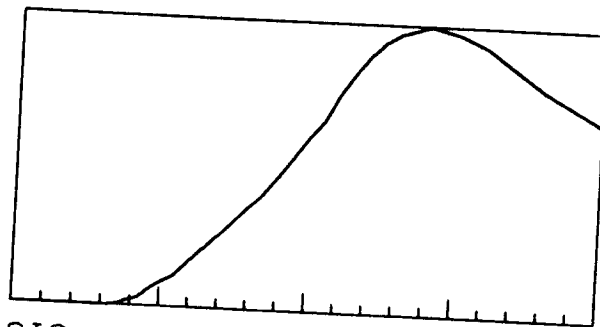
SIG*PHI



SIG*PHI



PHI



SIG

CF BASED ON WPP AND LANL
V-51(N,P)TI-51 PRESENT WORK

Figure 7.